ACS Catalysis

Research Article

pubs.acs.org/acscatalysis

Influence of Charge on the Reactivity of Supported Heterogeneous Transition Metal Catalysts

Liang Huang,[†,‡] Bo Han,[*,†] Yongjie Xi,[‡] Robert C. Forrey,[*,§] and Hansong Cheng[*,†,‡]

[†]Sustainable Energy Laboratory, China University of Geosciences Wuhan, 388 Lumo Road, Wuhan 430074, China

[‡]Department of Chemistry, National University of Singapore, 3 Science Drive 3, Singapore

[§]Department of Physics, Penn State University, Berks Campus, Reading, Pennsylvania 19610-6009, United States

Supporting Information

ABSTRACT: Nanoparticle catalysts consist of hundreds or thousands of atoms with structures that are essentially unknown. First-principles-based quantum mechanical calculations on this scale of substance would be prohibitively expensive to perform. Consequently, it has become common to use studies of small clusters at the subnano scale to gain insight into the chemical reactivity of nanoparticle catalysts. Recent theoretical and experimental investigations, however, have found that hydrogen reactivity on small Pt clusters is sensitive to the charge states of the clusters. This finding is in contrast to expectations about the reactivity of nanoparticles and casts doubt on whether small clusters can indeed be used to model realistic catalysts. The present case study for Pt clusters provides a systematic analysis of the charge sensitivity of the key catalytic properties for hydrogenation and clarifies the conditions for which a subnanoscale model may be expected to provide meaningful insights into the behavior of nanoparticle catalysts.

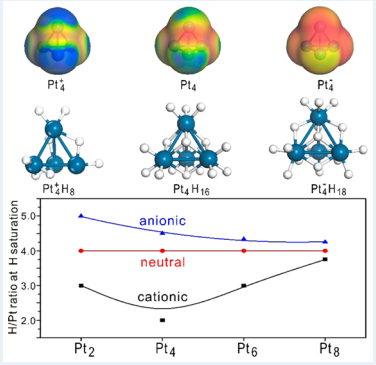

KEYWORDS: *platinum, subnano clusters, catalysts, hydrogenation, cluster charge states*

Nanoparticles of precious metals play an important role in heterogeneous catalytic reactions becaue of their excellent performance.[1−3] Gas phase metal clusters have been deemed to be versatile model systems for gaining a conceptual understanding of catalytic reaction mechanisms at a molecular level.[4−8] Dissociative chemisorption of hydrogen on platinum clusters is of particular importance because of the broad utilization of platinum in heterogeneous catalytic hydrogenation for a wide variety of industrial applications.[8−11] Although gas-phase platinum clusters have been a subject of intense research for many years, the intrinsic chemical reactivity of Pt clusters and the structures of the Pt hydride complexes are still not fully understood.[5,7,12,13]

Gas phase neutral, anionic, and cationic metal clusters have been produced by pulsed laser ablation[14−16] and from time-of-flight apparatus of supersonic beams via electron attachment or ionization.[17−20] After being thermalized to an ambient temperature through collisions with argon, these clusters enter a flow reactor channel, where they react with small molecules, such as CH_4, CO, N_2O, and NH_3. Activation of these molecules on the platinum clusters has led to the observation[21−28] that there are significant differences in physicochemical properties between neutral and ionic platinum clusters, which goes against the expectation that the outcome of a reaction on a catalyst nanoparticle should be little affected by a shortage or an excess of a few electrons. A recent combined theoretical and experimental study[29] on hydrogen dissociative chemisorption on small platinum clusters further showed that the number of hydrogen molecules adsorbed dissociatively on a cationic Pt cluster is significantly smaller than on a neutral cluster of the same size.[8,30,31] These experimental observations have raised a serious and fundamental question about whether a metal cluster in its charge state would maintain similar catalytic properties to the cluster in its charge-neutral form and, more profoundly, about whether clusters could, indeed, serve as a valid model for catalyst particles, regardless of their charge states. Considering that metal catalysts used in practice are normally charge-neutral and metal clusters produced in most spectroscopic experiments are either cationic or anionic, it is unlikely that this issue would be resolved through a direct experiment. The importance of this issue is further underscored by the possibility that the charge state of a metal catalyst on a supporting material may also be affected by the interaction between the catalyst and the substrate via electron transfer, which in turn may influence the activity of the catalyst.[32−34] Furthermore, recent studies have shown that electronically charged nanoparticles change their catalytic properties.[35] Therefore, it is desirable to understand the impact of charge on the reactivity of supported heterogeneous catalysts.

In this paper, we describe results of a theoretical study that attempts to determine whether a charged platinum cluster can serve as a credible model for a catalyst particle through a systematic analysis of the key catalytic properties for hydro-

Received: April 1, 2015
Revised: June 18, 2015
Published: June 23, 2015

DOI: 10.1021/acscatal.5b00689
ACS Catal. 2015, 5, 4592−4597

genation: H_2 dissociative chemisorption energy, sequential H desorption energy, charge transfer, H-mobility, and H-capacity. For neutral clusters, these properties were found to vary strongly with cluster size and H-coverage prior to reaching saturation.[8] The variation is greatly reduced at the saturation limit, which may be identified in molecular dynamics simulations when the H atoms recombine to form physisorbed H_2 molecules. In the present study, Pt_2, Pt_4, Pt_6, and Pt_8 clusters were selected as probes to systematically investigate the dependence of the catalytic properties on the charge state. The size effect of small Pt clusters and the appropriateness of using them to model nanoparticles are addressed by comparing the catalytic properties at full saturation to see whether there is a convergence pattern.

All calculations were performed using spin-polarization DFT/GGA with the PBE exchange-correlation functional[36] as implemented in the DMol^3 package.[37] A double numerical basis set augmented with polarization functions was used to describe the valence electrons, and core electrons were represented by an effective core pseudopotential. Charge analysis was performed on the basis of the Hirshfeld population distribution scheme.[38] Structures charged with +1 and −1, representing cationic and anionic clusters, respectively, were calculated to facilitate comparison of reactivity toward H_2 dissociative chemisorption. A transition state (TS) structural search using the LST/QST method[39] was performed to quantify the activation barriers of H_2 dissociation. The average dissociative chemisorption energy per molecule was evaluated using the equation:

$$\Delta E_{CE} = 2(E_{Pt_n} + m/2E_{H_2} - E_{Pt_nH_m})/m \quad (m = 2, 4, 6, ...) \tag{1}$$

where E_{Pt_n} represents the energy of the Pt_n cluster, E_{H_2} is the energy of the H_2 molecule, and $E_{Pt_nH_m}$ is the total energy of m hydrogen atoms adsorbed on the Pt_n cluster. For catalytic hydrogenation at a finite H_2 partial pressure, the capability of releasing a H atom from a catalyst surface with a high H/Pt ratio is paramount. Therefore, to quantitatively describe desorption of H atoms from a Pt cluster, the sequential desorption energy per atom is defined as

$$\Delta E_{DE} = E_H - (E_{Pt_nH_m} - E_{Pt_nH_{m-2}})/2 \quad (m = 2, 4, 6, ...) \tag{2}$$

where E_H is the energy of a H atom. At the full saturation limit, the sequential desorption energy ΔE_{DE} represents the threshold energy required for one H atom to desorb from the cluster. To determine whether a Pt cluster is fully saturated, we performed room temperature ab initio molecular dynamics (MD) simulations[40] to ensure all H atoms remain chemisorbed. The MD simulations were performed for 2 ps with a time step of 1 fs in a NVT canonical ensemble using the Nosé−Hoover thermostat. An excess of H atoms on the cluster generally results in recombination of surface H atoms into H_2 molecules physisorbed on the cluster upon the MD runs.

Neutral Pt_4, cationic Pt_4^+, and anionic Pt_4^- clusters were chosen as initial probes to identify the differences upon sequential H_2 dissociative chemisorption. All bare clusters, regardless of their charge state, adopt a tetrahedral configuration with essentially negligible structural deformation. The average bond distance is gradually elongated from 2.654 Å in the cationic state to 2.684 Å in the neutral state, and further increased to 2.728 Å in the anionic state. The calculated electron density difference of the neutral and charged states of Pt_4 and the d-band center of Pt clusters with various sizes and charges are shown in Figure 1. Figure 1a indicates that Pt_4^+ is

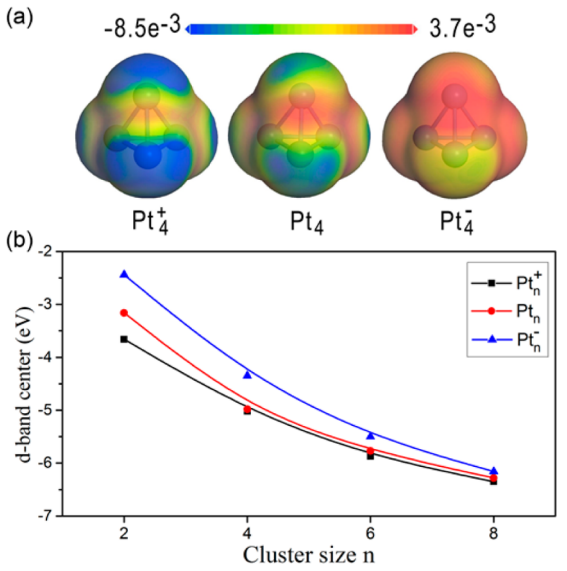

Figure 1. (a) The calculated electron density difference of Pt_4^+, Pt_4 and Pt_4^- clusters. (b) The d-band center of the Pt clusters with various sizes and charges.

most electron-deficient, and Pt_4^- is most charge-abundant. The charge distribution on the clusters will profoundly influence their capability to interact with hydrogen. Figure 1b reveals that the d-band center decreases gradually with the cluster size. In general, for a given cluster size, an anionic cluster exhibits a higher d-band center, whereas a cationic cluster displays a lower d-band center. However, the d-band center gradually converges as the cluster size increases, regardless of the charges on the clusters. Our results also suggest that the d-band center of large clusters becomes insensitive to the charge states.

To understand the influence of the electron density differences on catalytic dissociation of H_2, minimal energy pathway calculations of H_2 dissociative chemisorption were carried out on the Pt_4^+, Pt_4 and Pt_4^- clusters, respectively, as shown in Figure 2. For neutral Pt_4, spontaneous dissociation of the H_2 molecule on the atop-site of Pt_4 takes place upon contact of H_2 with the cluster (Figure 2a), leading to two atomic H species adsorbed on the same Pt atom. Although the process is highly exothermic, this site (R1) is not the most stable chemisorption configuration. In fact, the H atoms exhibit high mobility in the hydride complex, and one H atom can easily diffuse to bridge-site (P1) with a moderate activation barrier to further enhance the binding. The strong chemisorption arises from the orbital overlap between the 1s orbital of H and the 5d orbitals of the Pt atoms, resulting in electron transfer from Pt to H. As the H atom moves from R1 to P1, charge transfer from the Pt_4 cluster to the H atoms increases further by about 30%. H_2 dissociation on the electron rich anionic Pt_4^- cluster follows a similar reaction pathway (Figure 2c), but with a stronger interaction.

Figure 3 compares the calculated energy diagrams for the Pt_4^+, Pt_4 and Pt_4^- clusters. For the Pt_4 and Pt_4^- clusters, dissociation of H_2 is catalyzed by electron migration from d

DOI: 10.1021/acscatal.5b00689
ACS Catal. 2015, 5, 4592−4597

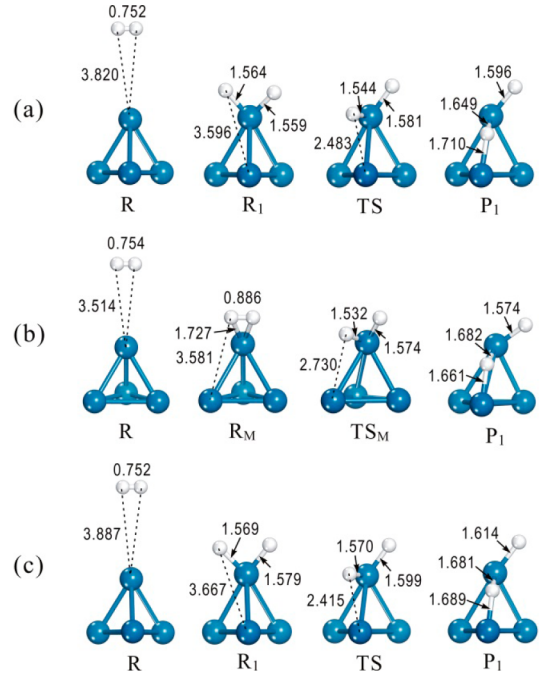

Figure 2. Reaction pathway of H_2 activated by (a) Pt_4 cluster, (b) Pt_4^+ cluster, and (c) Pt_4^- cluster. The unit for the bond length/distance is angstroms.

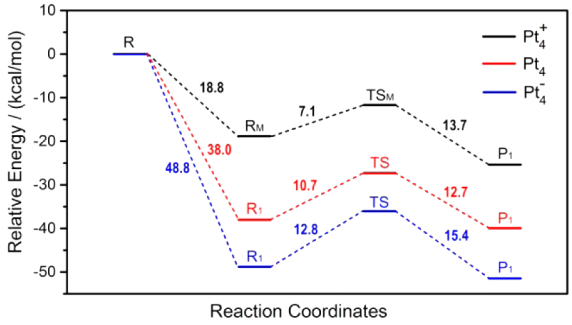

Figure 3. Calculated energy diagram of dissociative chemisorption of a H_2 molecule and the subsequent migrations of the H atoms on the Pt_4 clusters.

orbitals of the metal to the antibonding σ^* orbital of H_2. For the electron-deficient cationic Pt_4^+ cluster, a small electron transfer from the bonding σ-orbital of H_2 to the metal cluster is observed, and the force to break up the H_2 molecule is considerably weaker. In fact, the H_2 molecule may be molecularly anchored on Pt_4^+ upon contact with the cluster (Figure 2b). The molecularly bonded H_2 with a H−H bond distance of 0.886 Å is chemisorbed and slightly activated. A similar phenomenon of molecular H_2 adsorption on a cationic Ni_4^+ cluster has been observed previously in a vibrational spectroscopic (IR-MPD) study complemented with DFT calculations by Swart and co-workers.[41] In the present case, the calculated adsorption energy on the cationic Pt_4^+ cluster (−18.8 kcal/mol) is considerably weaker than the value on the atop-site of the neutral Pt_4 cluster (−38.0 kcal/mol). The molecularly adsorbed H_2 species (R_M) must overcome an energy barrier of 7.1 kcal/mol to be dissociated into two H atoms, which subsequently migrate to the most stable chemisorption sites on the Pt_4^+ cluster (P1). The adsorption is further enhanced by 6.6 kcal/mol upon the H−H bond break. Our calculations suggest that H migration on Pt_4^+ is easier than on Pt_4 because of the weaker binding on the cationic cluster. The calculated charge distribution indicates that the H atoms gain only a small fraction of an electron (0.046 e) from the Pt_4^+ cluster at the most stable binding sites (P1), consistent with the weaker adsorption strength relative to the case of neutral cluster. In contrast, the excess electron on Pt_4^- gives rise to significantly enhanced electron transfer from Pt_4^- to the H atoms (0.242e at P1), which is almost twice the value found for the neutral case. As a consequence, the dissociation process for Pt_4^- becomes highly exothermic, with a calculated chemisorption energy of −48.8 kcal/mol. Not surprisingly, the stronger interaction causes diffusion of H atoms on the anionic cluster to be slightly more restricted. An activation barrier of 12.8 kcal/mol, which is larger than for Pt_4 and Pt_4^+, is required to move a H atom to the most stable site (P1).

The above discussion describes results that are very sensitive to the charge state of the cluster. Although these results are consistent with experiments on small clusters, they provide limited insight into the reactivity of a realistic catalyst. In a typical hydrogenation reaction, a given hydrogen partial pressure is maintained, and the catalyst is saturated with hydrogen atoms. To address the effect of H coverage on Pt clusters with different charges, we examined the sequential dissociative chemisorption of H_2 molecules on the clusters up to full saturation. All of the H_2 molecules were completely dissociated into H atoms and then preferentially populated on the most favorable adsorption sites. For the Pt_4^+, Pt_4, and Pt_4^- clusters, saturation is realized at 8, 16, and 18 H atoms, respectively. The saturation limit for each of these clusters was thoroughly tested by performing MD simulations at room temperature. Figure 4 shows that loading two more H atoms onto the saturated clusters yields a H_2 molecule (peak at ∼0.8 Å) weakly bonded to the clusters. These results indicate that the charge state of a Pt cluster significantly affects the H-capacity of the cluster, which is one of the most important properties of a catalyst. The capacity increases with the number of electrons for a given cluster size. It is particularly noteworthy that the H-capacity of the cationic Pt_4^+ cluster is half of the value of the neutral cluster. A recent study by Kerpal and co-workers[29] reported that the H capacity of Pt_4^+ is higher than our result (12 vs 8); however, their reported $Pt_4H_{12}^+$ contains 3 molecularly bonded H_2 molecules and 6 dissociatively bonded H atoms, yielding an atomic H-capacity close to our result (6 vs 8). Because the main objective of a catalytic reaction in a hydrogenation process is the breaking of the H_2 bond, the Pt_4^- cluster would provide the highest catalytic reactivity, whereas the Pt_4^+ cluster with the significantly reduced H-capacity would yield the lowest activity.

The high sensitivity of the H-capacity to the charge state indicates that a Pt_4 cluster is too small to effectively represent a nanoparticle catalyst. To gain additional insight into the variation of the H-capacity for the different charge states, we calculated the average chemisorption energy, desorption energy, and charge transfer as a function of H coverage for the Pt_4^+, Pt_4, and Pt_4^- clusters. The results are shown in Figure 5. Clearly, the chemisorption energy decreases monotonically as H coverage increases, and thus, thermodynamically, dissociation of H_2 becomes increasingly more difficult. Despite the distinctive difference in H-capacities of these clusters, all of the calculated average chemisorption energies at full H saturation fall into a narrow range (∼24−26 kcal/mol). These results suggest that all 3 clusters to some extent hold

DOI: 10.1021/acscatal.5b00689
ACS Catal. 2015, 5, 4592−4597

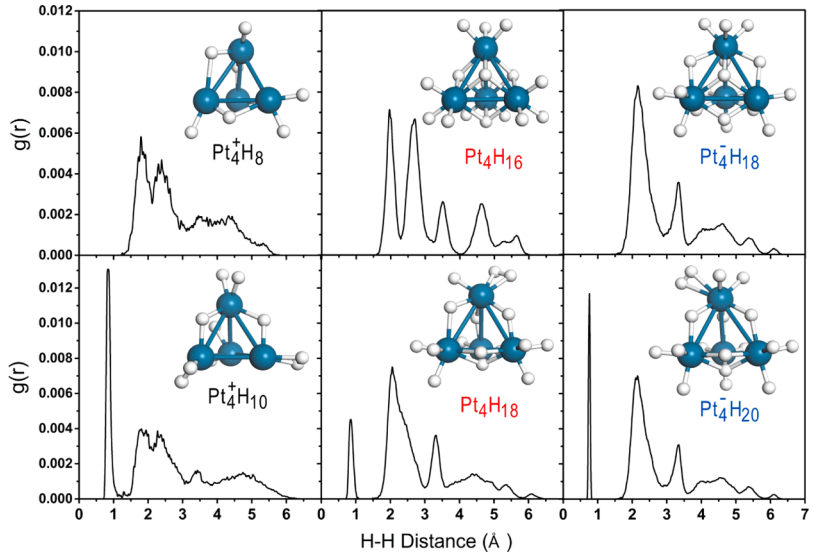

Figure 4. Calculated H−H distance distribution function $g(r)$ of full H saturated structures, obtained by tabulating all the H−H distances at each step of the MD trajectories.

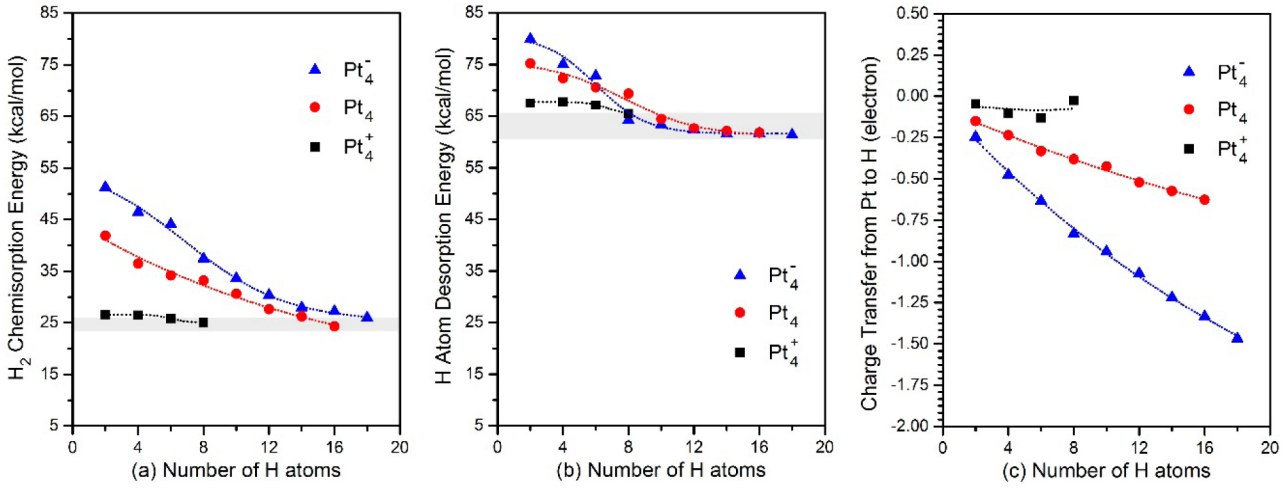

Figure 5. (a) The calculated H_2 average dissociative chemisorption energy, (b) H sequential desorption energy, and (c) loss of Hirshfeld charges of Pt clusters vs H coverage.

the same bonding strength toward H atoms at high H loadings. Likewise, all of the calculated desorption energies at full H coverage fall within a narrow range (~61−66 kcal/mol), despite the large energy variation observed at low H loadings. Although the chemisorption energies and H desorption energies on different charged Pt clusters are similar at full H saturation, the charge transfers shown in Figure 5c and Table S1 are quite different. This difference is responsible for the significant variation in H-capacity for the different charge states of the Pt_4 cluster.

To understand the effect of charge states on the H-capacity for different cluster sizes, we further calculated the saturated hydrogen complexes of Pt_2, Pt_6, and Pt_8 clusters with different charge states at full saturation. The H saturated hydride structures and amounts of fully saturated H atoms are shown in the Support Information (Figure S1 and Table S2), and the H/Pt ratio vs clusters size at full saturation is shown in Figure 6. In general, we find that more H atoms are loaded onto an anionic Pt_n^- cluster and fewer H atoms are attached to a cationic Pt_n^+ cluster; however, the variation decreases with cluster size. A constant H/Pt ratio of 4.00 for neutral Pt_n clusters is observed, regardless of the cluster size. For the anionic Pt_n^- cluster, the H/Pt ratio decreases from 5.00 to 4.25 as the clusters size

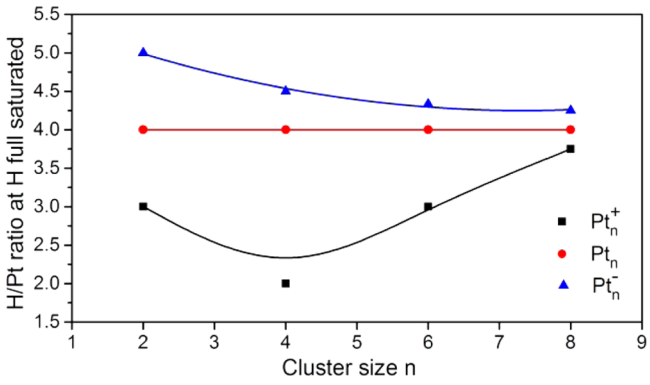

Figure 6. H/Pt ratio versus cluster size at full saturation. The H-capacity of the different charged clusters become similar to the neutral cluster when the cluster size reaches 8 atoms.

DOI: 10.1021/acscatal.5b00689
ACS Catal. 2015, 5, 4592−4597

increases from 2 to 8. For cationic Pt_n^+ clusters, the H/Pt ratio initially decreases with cluster size before increasing from 2.00 to 3.75 as the cluster size increases from 4 to 8. The H/Pt ratio gradually converges to 4.00 when the cluster size increases, independent of the charges on the clusters. Therefore, the charge effect would be significantly reduced with increasing cluster size at high H loadings. It is in this limit (H/Pt ratio equal to 4 at full H saturation) that a small cluster may be used to model nanoparticle catalysts. In this limit, the cationic or anionic charge can be readily dispersed and enough Pt−H bonds are involved to average the interaction between cluster and H atoms. This phenomenon is consistent with experiments for cationic Pt and Ni clusters, in which the reactivity of metal clusters was observed to increase significantly as the cluster size increases at subnano scale.[29,41] The reason for the increased catalytic reactivity is attributed mainly to the increased H-capacity for large cationic clusters in which the charge effect is effectively minimized. Our results demonstrate that the H-capacities on different charged clusters become similar when the cluster size increases, and the reactivity of a fully saturated cluster is no longer sensitive to its charge state when the cluster size exceeds a relatively small number of atoms (e.g., ∼ 8 Pt atoms).

Although 8 Pt atoms appears to be the minimum cluster size where the key catalytic properties for cationic, anionic, and neutral clusters converge, it should be noted that Pt−H interactions by themselves cannot directly predict the reactivity of Pt clusters toward hydrogenation reactions. Therefore, we studied the impact of the different charges for the hydrogenation of ethylene on H-saturated Pt clusters. For simplicity, a reactive process based on the Eley−Rideal mechanism rather than the more commonly assumed Langmuir−Hinshelwood mechanism was used as the model based on the following considerations. In a typical hydrogenation reaction, the ethylene pressure is usually kept lower than that of hydrogen,[42] and thus, it is likely that the Pt_n catalyst is fully saturated with hydrogen atoms, considering the facile H_2 dissociation on the cluster. In addition, the size of the clusters used in the present study is relatively small, and thus, it is difficult to accommodate a coadsorption structure of H atoms and ethylene, which is a model needed for describing the Langmuir−Hinshelwood mechanism. The Langmuir−Hinshelwood process is best described with a surface or a large cluster model, which is, however, not the main emphasis of the present study. The calculated results are shown in Figure 7 and Table S3. Interestingly, the activation energies for the three types of clusters do not show the same convergence pattern with cluster size. Despite having nearly identical desorption energies at saturation, the anionic Pt_8 cluster has a barrier for hydrogenation of ethylene that is nearly twice that of the neutral and cationic Pt_8 clusters. The strong variation in reaction energy with cluster size and the lack of correlation to activation energy is due to the structural relaxation that occurs for small clusters after reaction.

The present study for Pt clusters provides a systematic analysis of the charge sensitivity of the key catalytic properties for hydrogenation and clarifies the conditions for which a subnanoscale cluster model may be expected to provide meaningful insights into the behavior of nanoparticle catalysts. The results show that the dissociation of H_2 is strongly correlated to the charge state of Pt clusters at low H coverage. In a typical hydrogenation reaction, however, a constant pressure of hydrogen is normally maintained. Consequently,

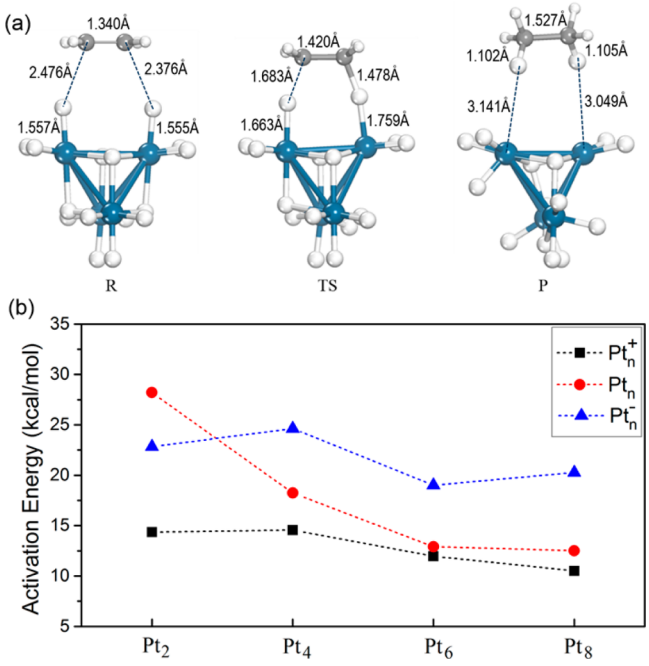

Figure 7. Hydrogenation of ethylene on H-saturated Pt clusters: (a) minimum energy configurations for H-saturated Pt_4 cluster and (b) activation energies as a function of charge state and cluster size.

the surface of a catalyst particle is expected to be fully covered by either molecular or atomic hydrogen. Because the amount of H atoms at full saturation for small anionic clusters is much higher than that of neutral and cationic clusters, the negatively charged particles may provide more H atoms during a hydrogenation process, leading to a faster reaction rate for systems with similar activation energies. Hydrogenation of ethylene has an activation energy for anionic Pt clusters that is ∼0.5 eV greater than for neutral or cationic Pt clusters, which suggests that there are also competing mechanisms for small clusters that may affect the kinetics. Our calculations indicate that the catalytic behavior of Pt clusters in their charge states becomes similar to that of the corresponding neutral clusters at full H saturation when the cluster size is increased beyond an appropriate limit. Only in that limit may a relatively small saturated cluster be used to represent a nanoscale metal catalyst. These findings should provide useful insight for the design of catalysts with a core−shell or supported structure, in which the charge state of the catalyst particle is determined by the interaction between catalyst and substrate materials. It should also be useful for the cluster community that has been using charged clusters as a model for catalysts for years because a charge, either cationic or anionic, is needed for their time-of-flight supersonic beam experiments.

■ ASSOCIATED CONTENT

Supporting Information

The Supporting Information is available free of charge on the ACS Publications website at DOI: 10.1021/acscatal.5b00689.

Additional tables and figures (PDF)

■ AUTHOR INFORMATION

Corresponding Authors

*E-mail: hanbo@cug.edu.cn.

*E-mail: rcf6@psu.edu.

DOI: 10.1021/acscatal.5b00689
ACS Catal. 2015, 5, 4592−4597

*E-mail: chghs2@gmail.com.

Notes

The authors declare no competing financial interest.

■ ACKNOWLEDGMENTS

We gratefully acknowledge support of the research by a NUS start-up grant, a Singapore National Research Foundation POC grant, and the Singapore-Peking-Oxford Research Enterprise, COY-15-EWI-RCFSA/N197-1. Support from the National Natural Science Foundation of China (No. 21473164, 21203169 and 21233006), the Fundamental Research Funds for the Central Universities, China University of Geosciences, and the United States National Science Foundation (No. PHY-1203228) is also gratefully acknowledged.

■ REFERENCES

(1) Tao, F.; Grass, M. E.; Zhang, Y.; Butcher, D. R.; Renzas, J. R.; Liu, Z.; Chung, J. Y.; Mun, B. S.; Salmeron, M.; Somorjai, G. A. *Science* **2008**, *322*, 932−934.
(2) Lim, B.; Jiang, M.; Camargo, P. H.; Cho, E. C.; Tao, J.; Lu, X.; Zhu, Y.; Xia, Y. *Science* **2009**, *324*, 1302−5.
(3) Imaoka, T.; Kitazawa, H.; Chun, W. J.; Omura, S.; Albrecht, K.; Yamamoto, K. *J. Am. Chem. Soc.* **2013**, *135*, 13089−95.
(4) Lang, S. M.; Bernhardt, T. M. *Phys. Chem. Chem. Phys.* **2012**, *14*, 9255−69.
(5) Kumar, V.; Kawazoe, Y. *Phys. Rev. B: Condens. Matter Mater. Phys.* **2008**, *77*, 205418.
(6) Harding, D. J.; Kerpal, C.; Rayner, D. M.; Fielicke, A. *J. Chem. Phys.* **2012**, *136*, 211103.
(7) Xiao, L.; Wang, L. *J. Phys. Chem. A* **2004**, *108*, 8605−8614.
(8) Zhou, C.; Wu, J.; Nie, A.; Forrey, R. C.; Tachibana, A.; Cheng, H. *J. Phys. Chem. C* **2007**, *111*, 12773−12778.
(9) Schmidt, E.; Vargas, A.; Mallat, T.; Baiker, A. *J. Am. Chem. Soc.* **2009**, *131*, 12358−12367.
(10) Chen, A.; Holt-Hindle, P. *Chem. Rev.* **2010**, *110*, 3767−3804.
(11) Huda, M. N.; Kleinman, L. *Phys. Rev. B: Condens. Matter Mater. Phys.* **2006**, *74*, 195407.
(12) Ankudinov, A.; Rehr, J.; Low, J.; Bare, S. *Phys. Rev. Lett.* **2001**, *86*, 1642−1645.
(13) Sebetci, A. *Phys. Chem. Chem. Phys.* **2009**, *11*, 921−5.
(14) Koszinowski, K.; Schröder, D.; Schwarz, H. *J. Phys. Chem. A* **2003**, *107*, 4999−5006.
(15) Swart, I.; Fielicke, A.; Redlich, B.; Meijer, G.; Weckhuysen, B. M.; de Groot, F. M. F. *J. Am. Chem. Soc.* **2007**, *129*, 2516−2520.
(16) Swart, I.; de Groot, F. M. F.; Weckhuysen, B. M.; Gruene, P.; Meijer, G.; Fielicke, A. *J. Phys. Chem. A* **2008**, *112*, 1139−1149.
(17) Wang, L. S.; Cheng, H. S.; Fan, J. W. *J. Chem. Phys.* **1995**, *102*, 9480−9493.
(18) Hakkinen, H.; Yoon, B.; Landman, U.; Li, X.; Zhai, H. J.; Wang, L. S. *J. Phys. Chem. A* **2003**, *107*, 6168−6175.
(19) Castleman, A. W.; Keesee, R. G. *Chem. Rev.* **1986**, *86*, 589−618.
(20) Deheer, W. A. *Rev. Mod. Phys.* **1993**, *65*, 611−676.
(21) Shi, Y.; Ervin, K. M. *J. Chem. Phys.* **1998**, *108*, 1757.
(22) Achatz, U.; Berg, C.; Joos, S.; Fox, B. S.; Beyer, M. K.; Niedner-Schatteburg, G.; Bondybey, V. E. *Chem. Phys. Lett.* **2000**, *320*, 53−58.
(23) Balteanu, I.; Petru Balaj, O.; Beyer, M. K.; Bondybey, V. E. *Phys. Chem. Chem. Phys.* **2004**, *6*, 2910−2913.
(24) Adlhart, C.; Uggerud, E. *Chem. Commun.* **2006**, 2581−2.
(25) Kummerlöwe, G.; Balteanu, I.; Sun, Z.; Balaj, O. P.; Bondybey, V. E.; Beyer, M. K. *Int. J. Mass Spectrom.* **2006**, *254*, 183−188.
(26) Oncak, M.; Cao, Y.; Hockendorf, R. F.; Beyer, M. K.; Zahradnik, R.; Schwarz, H. *Chem. - Eur. J.* **2009**, *15*, 8465−74.
(27) Harding, D. J.; Kerpal, C.; Meijer, G.; Fielicke, A. *Angew. Chem., Int. Ed.* **2012**, *51*, 817−9.
(28) Lv, L.; Wang, Y.; Wang, Q.; Liu, H. *J. Phys. Chem. C* **2010**, *114*, 17610−17620.
(29) Kerpal, C.; Harding, D. J.; Rayner, D. M.; Fielicke, A. *J. Phys. Chem. A* **2013**, *117*, 8230−7.
(30) Szarek, P.; Urakami, K.; Zhou, C.; Cheng, H.; Tachibana, A. *J. Chem. Phys.* **2009**, *130*, 084111.
(31) Chen, L.; Cooper, A. C.; Pez, G. P.; Cheng, H. *J. Phys. Chem. C* **2007**, *111*, 5514−5519.
(32) Helali, Z.; Markovits, A.; Minot, C.; Abderrabba, M. *Chem. Phys. Lett.* **2013**, *565*, 45−51.
(33) Campbell, C. T. *Nat. Chem.* **2012**, *4*, 597−598.
(34) Bruix, A.; Rodriguez, J. A.; Ramirez, P. J.; Senanayake, S. D.; Evans, J.; Park, J. B.; Stacchiola, D.; Liu, P.; Hrbek, J.; Illas, F. *J. Am. Chem. Soc.* **2012**, *134*, 8968−8974.
(35) Carrettin, S.; Concepción, P.; Corma, A.; López Nieto, J. M.; Puntes, V. F. *Angew. Chem., Int. Ed.* **2004**, *43*, 2538−2540.
(36) Perdew, J. P.; Burke, K.; Ernzerhof, M. *Phys. Rev. Lett.* **1996**, *77*, 3865−3868.
(37) Delley, B. *J. Chem. Phys.* **2000**, *113*, 7756−7764.
(38) Hirshfeld, F. L. *Theor. Chim. Acta* **1977**, *44*, 129−138.
(39) Halgren, T. A.; Lipscomb, W. N. *Chem. Phys. Lett.* **1977**, *49*, 225−232.
(40) Martyna, G. J.; Tuckerman, M. E.; Tobias, D. J.; Klein, M. L. *Mol. Phys.* **1996**, *87*, 1117−1157.
(41) Swart, I.; Gruene, P.; Fielicke, A.; Meijer, G.; Weckhuysen, B. M.; de Groot, F. M. *Phys. Chem. Chem. Phys.* **2008**, *10*, 5743−5.
(42) Cremer, P. S.; Su, X.; Shen, Y. R.; Somorjai, G. A. *J. Am. Chem. Soc.* **1996**, *118*, 2942−2949.

DOI: 10.1021/acscatal.5b00689
ACS Catal. 2015, 5, 4592−4597